

Light Weight Plasters Containing Vermiculite and FGD Gypsum Wastes for Sustainable and Energy Efficient Building Construction Material

Dr. Soumitra Maiti

CSIR-CBRI

Dr. Neeraj Jain

CSIR-CBRI

Dr. Jaideep Malik

CSIR-CBRI

Aakriti - (✉ aakriti860@gmail.com)

CSIR-CBRI

Research Article

Keywords: FGD gypsum, light weight plaster, GVP, acoustic properties, thermal conductivity

Posted Date: March 16th, 2023

DOI: <https://doi.org/10.21203/rs.3.rs-2303609/v2>

License:   This work is licensed under a Creative Commons Attribution 4.0 International License.

[Read Full License](#)

Additional Declarations:

Tables 1-6 is available in the Supplementary Files section.

Light Weight Plasters Containing Vermiculite and FGD Gypsum Wastes for Sustainable and Energy Efficient Building Construction Material

Abstract: Development of lightweight plasters for mortar rendering utilizing Flue gas desulfurization (FGD) gypsum have been reported here. Lightweight plasters prepared using FGD gypsum and exfoliated vermiculite were characterized and studied in detail for interior wall applications. Different gypsum vermiculite plasters (GVP) with variable amounts of vermiculite were characterized by X-ray diffraction (XRD), scanning electron microscopy (SEM) and thermal gravimetric analysis (TG-DTG). The physicochemical and mechanical properties of all the samples are determined and considered to be efficient for interior applications. An optimum mix composition was selected based on its compressive strength, water absorption and porosity. Water absorption and porosity studies restrict the usage of GVP only to interior wall purposes. The acoustic performance of the materials revealed good sound absorption ($\alpha = 0.65$). Plasters exhibit satisfactory durability under severe conditions of winter and summer weather. GVP shows excellent fire resistance under BS 476-1997 fire resistance classification with thermal conductivities (< 0.161 W/mK) much lower than standard building materials, which makes them fit for energy efficient insulation materials. These studies depict the efficient utilization of thermal power plant waste, FGD gypsum in interior wall insulation for mortar rendering and can be further extended to exterior construction applications by reducing water absorption.

Keywords: FGD gypsum, light weight plaster, GVP, acoustic properties, thermal conductivity.

1. Introduction

Flue Gas Desulfurization Gypsum (FGDG) is obtained from coal-based electric power plants. Burning of coal produces harmful flue gases like CO_2 , NO_x , and SO_x . SO_x is removed from the flue gases by the process of desulfurization via different techniques. Scrubbing method is most extensively used for the process of desulfurization. 'Wet-type scrubbing process' and 'dry or Semi-Dry scrubbing process' are generally two scrubbing methods. Among them 'Wet-type scrubbing' is the most widely used technique for desulfurization [1,2]. The chemical composition of FGD gypsum is $\text{CaSO}_4 \cdot 2\text{H}_2\text{O}$, identical to natural gypsum. Chemical reactions involved in the process of conversion of SO_2 gas into FGD gypsum is as follows [3,4,5]-



In this process, slurry of lime or limestone, which is forced oxidized used as a sorbent for sulfur dioxide and results in the generation of FGD gypsum. Due to the huge available amounts of FGD gypsum, it needed to be placed in disposal areas. This process is expensive as well as causes various kinds of pollution problems [6]. The FGD gypsum's composition is comparable to that of natural gypsum in terms of CaO and SO_3 , although it contains less Al_2O_3 and Fe_2O_3 . This is because the FGD gypsum lacks the clays and iron minerals found in the natural material [7].

According to a CSE report, India is about to become the largest emitter of SO_2 in the world by replacing China, as its emission has increased by 50% in the last decade. In order to prevent this extreme situation, a significant share

37 (90%) of India's thermal power capacity is likely to opt for wet limestone FGD technology due to its well-proven
38 operational and technological track record across the world. It is estimated that after the installation of FGD units,
39 India's power plants would produce around 12–17 million tonnes of gypsum by 2022 with a consumption 32,000
40 tonnes of limestone per annum by a 500 MWh unit. Under this scenario, the unit would produce 54–60,000 tonnes of
41 gypsum per annum. At this rate of generation, FGDG stockpiled and due to its ability to absorb toxic elements like F,
42 As, Hg, Cd, Cr and Pb etc. [8] will be pernicious to the environment and possess detrimental effects to land, water and
43 air. Therefore, it is necessary to explore the utilization potential of this waste material, as it can be beneficial for both
44 the economy and the environment.

45 Gypsum is an integral component of cement production and the sector relied on costly imported or poor quality
46 synthetic gypsum. Gypsum is a soluble source of essential plant nutrients like calcium and sulfur and can improve
47 overall plant growth [9]. Gypsum amendments improve the physical properties of some soils (especially heavy clay
48 soils) [10,11]. It helps reduce erosion losses of soils and nutrients, and the concentrations of soluble phosphorus in
49 surface water runoff. FGD gypsum is being used in agriculture in US and China. Since ancient times, gypsum has also
50 been used as a building material due to its unique hydration and dehydration property. It is well known that gypsum
51 building materials are light weight, provide thermal insulation, fire resistance [12] and possess good acoustic properties.
52 Moreover, rapid population growth and urbanization have increased demand for raw materials such as cement and
53 aggregates many folds in the construction industry worldwide. The mission of sustainable development has led to
54 pressure to improve environmental performance in the construction process by reducing consumption of natural
55 resources extracted.

56 Researchers around the world utilized FGD gypsum for the production of various kinds of value added building
57 materials such as wallboard [1,13], blocks [14,15], tiles [16,17] etc., after conversion into β -hemihydrate gypsum.
58 Several researchers demonstrated the procedure for the production of structural board from FGD gypsum. A process
59 for the production of a multilayer thermal insulating board containing different power plant coal residues such as Fly
60 ash, FGD gypsum etc., has been patented. FGD gypsum has also been used in mixtures applied as fire proof coatings
61 for steel structures [18]. Apart from its use in wallboard products, research also has been carried out on the
62 development of FGD gypsum markets mainly in two areas: (a) as an admixture in cement and (b) agriculture uses,
63 such as a soil amendment. Thus, utilization of waste gypsum (FGD) offers not only the solution of disposal problems,
64 but also help to save cement, reduce carbon foot prints by reducing green house gases emission, conserve natural
65 resources for meeting increased demand of aggregates and save energy and environment. Additives are typically
66 incorporated into the gypsum matrix to improve the material's insulating qualities and increase its fire resistance. The
67 most common additions used for fire protection include vermiculite, mica, alumina, perlite, and ceramic hollow
68 spheres [19,20]. Vermiculite, a mineral that resembles mica and has sparkling flakes, belongs to the phyllosilicate
69 family. When heated between 650 and 950°C, it expands up to 30 times its original volume [21]. Vermiculite's physical
70 characteristics may vary depending on how its chemical composition changes [22]. Due to the apparent volume
71 expansion following high-temperature calcining, vermiculite is a type of multi-layered silicate rock with a very high
72 specific surface area. Vermiculite undergoes numerous cycles of interlayer water release during the calcining process
73 before becoming expanded vermiculite (EV), which has a highly porous structure [23]. EV is suitable for a wide range

74 of applications across a variety of fields due to its low thermal conductivity, low bulk density, relatively high
75 refractoriness, chemical inertness durability, and environmental safety. Increased workability, reduced unit weight,
76 improved sound and thermal insulation, and improved fire resistance are all benefits of employing EV in the matrix
77 [24]. These facts justify the use of vermiculite as a construction material and simultaneously as a heat isolation and
78 sound absorption material [25,26] Gypsum plasters' 28-day compressive strength was reported to be reduced by
79 19.46% and 32.22%, respectively, with the addition of 10% and 20% EV (size 0.145 mm). On the other hand, the 28-
80 day bending strength was improved by 16.25% and 35%, respectively, with the addition of 10% and 20% EV [27]. It
81 has been also reported that the addition of EV at values ranging from 5% to 25%, by weight, decreased the mechanical
82 strength of fibrous gypsum plasters. As the EV content increases, this reduction also increases [28]. The tiles have
83 been manufactured from cement and exfoliated vermiculite and the EV incorporation was 5-50%. According to the
84 findings, the amount of exfoliated vermiculite decreased with increasing compressive strength and flexural strength
85 [29]. Raw, inert materials of various densities have been widely used and known for producing lightweight cements.
86 Lightweight aggregates like expanded perlite and vermiculite, among others, are typically combined with gypsum and
87 cement to lessen the density of the finished product [30]. In order to create a novel lightweight plaster material with
88 improved thermal qualities for industrial uses in accordance with building rules, the compatibility of polyamide
89 powder waste with plaster has been investigated [31].

90 In the present work, we proposed to develop light weight plaster with FGD gypsum using vermiculite for
91 rendering work in the construction industry. Several mixes of β -hemihydrate gypsum and exfoliated vermiculite were
92 envisaged in different proportions to develop light weight gypsum vermiculite plasters (GVP). Raw FGD gypsum was
93 calcined to obtain β -hemihydrate form. The gypsum vermiculite plasters with vermiculite content of 3, 4, 5, 8, 10 &
94 12% were casted into cubes and studied for their mechanical properties such as compressive and flexural strength.
95 The cubes were characterized by X-ray diffraction (XRD), scanning electron microscopy (SEM) and thermal
96 gravimetric analysis (TG-DTG). GVP samples were investigated for their water absorption, porosity, thermal
97 conductivity, fire resistance, acoustic properties and durability under severe environments.

98 **2. Materials & Methods**

99 **2.1 Raw materials**

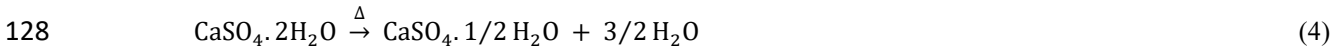
100 Different mix compositions of FGD gypsum (FGDG) and vermiculite were used for the development of light
101 weight plaster. FGDG was procured from NTPC (National Thermal Power Corporation) operated coal-based power
102 plant, VSTPS (Vindhyachal Super Thermal Power Station) located in Singrauli, Madhya Pradesh. Vermiculite crystals
103 of grade, 1-2 mm (after grit removal) were used. Diethylenetriaminepentaacetic acid (DTPA) was used as a chemical
104 retarder to delay fast setting of binders. The FGDG sample is greyish in appearance and vermiculite particles reflect
105 light to dark brown particles. The collected samples of FGDG were sun dried, ball milled for an hour, and sieved
106 through a 90 μ m sieve prior to its various physical and chemical analyses as per IS: 1288-1982 [32]. The physical
107 properties of the materials are summarized in Table 1. These results suggest that FGDG conforms to the requirements
108 of IS: 12679-1989 [33]. A pycnometer was used to measure the specific gravity of the samples.

109 **2.2 Characterization**

110 Scanning electron microscopy (SEM; Carl Zeiss-Ultra plus55), powder X-ray diffraction (XRD; Bruker-D8
 111 Advance, Cu-K α) and thermogravimetry/ differential thermal analysis (TGA/DTA; EXSTAR, SII 6300) were used
 112 for characterization of the samples.

113 Microscopic images of FGDG show euhedral prismatic rod-like particles ranging from 1 μm to 200 μm in length
 114 without any sign of agglomeration. SEM images of exfoliated vermiculite depict flaky lamellar structures
 115 corresponding to multi-layered trioctahedral structure of vermiculite made of Mg-Fe-Al-Si. This lamellar structure
 116 contains air in-between layers that explain the exfoliation of the vermiculite [34]. XRD data of the materials were
 117 recorded on a RIGAKU 2200 diffractometer at 30 kV and 10 mA for Cu-K α ($\lambda = 1.54050 \text{ \AA}$), with a step size of 0.02°
 118 in 2θ . The XRD pattern of FGDG revealed that the main crystalline phases present are gypsum and CaO,
 119 corresponding to more than 90% of gypsum content determined by chemical analysis IS:1288-1999. XRD pattern of
 120 vermiculite shows major peaks of calcium magnesium aluminum silicate (#) at 27.59° , 29.92° , 35.10° , 35.46° and
 121 45.81° ; calcium aluminum silicate (*) peaks observed at 2θ of 9.44° and apart from it, a peak of quartz (Q) is also
 122 observed at 26.64° .

123 TGA/DTA has been realized to determine the phase stability and different species present in the materials. The
 124 weight loss as a function of temperature was determined using TGA and details of the experiment are given somewhere
 125 else [35]. TGA curve of FGDG sample shows two signatures of weight loss at $\sim 140^\circ\text{C}$ and $\sim 660^\circ\text{C}$ that signifies
 126 endothermic loss of $3/2$ moles of H_2O from calcium sulfate dihydrate to form calcium hemihydrate (Eqn. 4) and weight
 127 loss due to decomposition of carbonate content (Eqn. 5), respectively.



130 TGA curve of vermiculites accounts for 5% weight loss on heating upto 1000°C . Early weight loss $\sim 100^\circ\text{C}$
 131 accounted for the loss of surface absorbed water molecules. However, the majority of weight loss occurs between 500
 132 to 900°C , which could be a result of dehydration of chemically bound water molecules [36].

133 2.3 Mechanical Properties

134 The mechanical properties of all the mixes were determined as per IS: 2542-1978 (Part I) [37]. Setting times of
 135 pastes were determined using normal Vicat's apparatus according to IS: 2547-1976 (Part II) [38].

136 2.4 Water Absorption and Porosity

137 To determine water absorption and porosity of hemihydrate plaster, $25\text{mm} \times 25\text{mm} \times 25\text{mm}$ cubes were casted
 138 and treated as mentioned above [30,39]. The initial weight of the cubes was measured and then immersed in water for
 139 a particular period of 2, 8 and 24 hours, and their weight was measured again after each period to calculate the
 140 percentage of water absorption using the following expression-[40]

$$141 \quad \text{Water absorption (\%)} = \frac{W_2 - W_1}{W_1} \times 100 \quad (6)$$

142 where, W_1 is the initial weight of the specimen and W_2 is the weight of the specimen after immersion in water.

143 The porosity of the specimens was determined from the following expression-

$$144 \quad \text{Porosity} = \frac{W \cdot d_s}{d_w} \quad (7)$$

145 where, W is the weight loss, d_s is the dry density of the gypsum binder and d_w is the density of water used.

146 2.5 Thermal Conductivity Measurement

147 The guarded hot plate method was used to determine the thermal conductivities of GVP samples. It follows a
148 steady-state method that requires the specimen insulating material to be in equilibrium with its surroundings for
149 accurate measurements. The thermal conductivities of the GVP mixes were measured as per IS: 3346-1980 [41].
150 Finally, the thermal conductivity values of the GVP mixes were determined using the equation given below-

$$151 \quad \kappa = V \times I \times d / [2 \times A(T_H - T_C)] \quad (8)$$

152 where, κ , d , V , I , T_H and T_C are the thermal conductivity (in W/m.K), thickness of specimen (in mm), voltage (in V),
153 current (in A), temperature of hot-plate and cold-plate (in K), respectively.

154 2.6 Acoustic Properties

155 The acoustic performance of samples was measured on a Holmarc (ITA219) impedance tube system consisting
156 of an impedance tube, two microphone locations, and a digital frequency analysis. The acoustic transfer matrix is
157 calculated from the pressure and particle velocity, or the acoustic impedance of the traveling waves on either side of
158 the specimen. Transmission loss (TLN) and sound absorption coefficient (α_n) are extracted from this transfer matrix
159 using the following equations-

$$160 \quad TLN = 10 \log_{10} W_i / W_t \quad (9)$$

$$161 \quad \alpha_n = 1 - |\Gamma|^2 \quad (10)$$

162 where, W_i and W_t are the power of incident and transmitted sound. α_n , TLN and Γ are the sound absorption coefficient,
163 transmission loss and pressure reflection coefficient, respectively.

164

165 3. Results & Discussion

166 3.1 Mix proportions

167 The pre-treated FGD gypsum was used to generate calcium sulfate hemihydrate (β -hemihydrate), which is later
168 utilized to develop hemihydrate plaster and gypsum vermiculite plaster (GVP) as per standard methods. β -hemihydrate
169 was obtained by firing the FGDG at 150 – 155 °C for 3 – 4 hours with intermittent spatulation every 45 minutes to
170 obtain a uniform product. The XRD data of β -hemihydrate obtained after calcination is shown in Fig. 1a. It depicts
171 that after calcination, the major content of dihydrate gypsum gets converted to hemihydrate with major crystalline
172 peaks observed at 2θ values 14.74°, 25.66°, 29.71°, 31.87°, 42.23°, 49.31° and 54.11° are indexed for β -hemihydrate
173 plaster. XRD analysis reveals that β -hemihydrate content is about 85-88 % that matches well with similar findings
174 observed during chemical analysis. Unreacted gypsum and anhydrite form accounts for 4 – 6% and 5 – 8%,
175 respectively, with some traces of calcium oxide in the β -hemihydrate sample.

176 TG-DTG curve of β -hemihydrate plaster is shown in Fig. 1b, which exhibits a small (1.2%) mass loss at 86 °C
177 owing to removal of free water and an endotherm ~ 125 °C that accounts for 5.0% mass loss. This clearly indicates
178 that more than 90% of the FGD gypsum gets converted to hemihydrate form after calcination. . [The \$\text{CaSO}_4 \cdot 2\text{H}_2\text{O}\$](#)
179 [content was determined by the chemical analysis as per IS:2547-Part 2: 1976.](#) However, this 5.0% loss is due to the
180 inversion of remaining fully or partially dihydrated gypsum to hemihydrated plaster.

181 The gypsum vermiculite plaster (GVP) was developed from β -hemihydrate and vermiculite in different
182 compositions along with a suitable retarder (DTPA) to increase the setting time as per BIS 2542:1978. For mix
183 compositions, blending was carried out in a ribbon powder mixture for a desired interval of time to form a
184 homogeneous mixture. Several mix compositions of gypsum vermiculite plaster with varying percentages of
185 vermiculite (1.0 – 12.0%) were prepared. The composition of these trial mixtures is given in Table 2.

186 3.2 Physical and Chemical Properties of GVP

187 The 25 mm cubes of all GVP mixes were characterized for their chemical and physical properties as per IS:
188 2542-1978 [37]. The physical characteristics of the samples are given in Table 3 and 4.

189 3.3 Compressive and Flexural Strength

190 Compressive strength results of all the samples determined at 7 and 28 days of hydration are presented in Fig. 2.
191 It is observed that the compressive strength of all the samples increases with hydration period due to the completion
192 of the hydration reaction. However, on replacement of FGD gypsum with vermiculite, compressive strength reduces
193 gradually as we increase the percentage of vermiculite. GVP3 exhibits compressive strength of 12.6 MPa followed by
194 GVP4 > GVP5 > GVP 8 > GVP10 > GVP12 in order after 28 days. This is known to be attributed to lower gypsum
195 content and porous nature of vermiculite which results in poor compressive strength. Although the mixes with GVP0,
196 GVP1, and GVP2 showed the highest compressive strength, they failed to meet the minimum density requirement of
197 at least 750kg/m³ according to BIS: 2547-Part 2: 1976 for plaster. Flexural strength results of the samples show a
198 similar trend as observed for compressive test results. Flexural strengths of the GVP mixes are shown as a bar diagram
199 in Fig. 3.

200 3.4 SEM & XRD Analysis

201 SEM images of 28 days hydrated GVP3 plaster were captured and shown in Fig. 5. A perusal of SEM micrographs
202 shows intermingled vermiculite and gypsum particles that indicate an excellent interlocking of gypsum plaster crystals
203 with vermiculite granules. Due to this agglomeration, there observed a high bonding of the plaster, which ultimately
204 results in higher mechanical strength of GVP3 plaster.

205 XRD of hydrated gypsum vermiculite plaster is shown in Fig. 5a, which depicts major peaks of calcium sulfate
206 dihydrate (G) at 2θ of 11.69°, 20.78°, 23.45°, 29.17°, 33.42° etc. This shows that hemihydrate plaster gets converted
207 into dihydrate gypsum after hydration reactions, responsible for binding properties. Peaks of Calcium Magnesium
208 Aluminum Silicate (#) are observed at 29.01° and 31.23° along with peaks of Calcium Aluminum Silicate (*) peaks at
209 9.44° present in vermiculite.

210 TG-DTG curves of GVP-3 plaster are shown in Fig. 5b. There observed two prominent weight loss signatures
211 from the analysis of DTG curve. Major endothermic peak observed at 110 – 140 °C accounting for ~ 18% weight loss
212 corresponds to FGD gypsum due to dehydration of 3/2 moles of water. The second endotherm observed between 500
213 – 900 °C corresponds to weight loss attributable to vermiculite due to dehydration of chemically bound water
214 molecules.

215 The distribution of vermiculite particle in 28 days hydrated GVP3 and GVP 12 at different scale and
216 magnifications are shown in Fig. 4. A perusal of SEM micrographs shows euhedral prismatic, tabular and twined
217 shaped gypsum particle along with flaky lamellar structures of vermiculites. It was also noticed that vermiculite

218 particles are intermingled with gypsum particles that indicate an excellent interlocking of gypsum crystals with
219 vermiculite granules. In GVP3, a high bonding of the plaster with vermiculite is observed due to presence of higher
220 amount of gypsum, which ultimately results in higher mechanical strength of GVP3 plaster.

221 **3.5 Determination of Water Absorption and Porosity of GVP**

222 The calculated values of water absorption and porosity of the gypsum vermiculite plasters at 2, 8 and 24 h are
223 shown in Table 5. The results revealed that as the percentage of vermiculite increased from 1 to 12% in the plaster,
224 water absorption and porosity increased while the compressive strength and dry bulk density (powder) decreased. The
225 above observations are in good agreement with Martias *et al.* and Gencel *et al.* [43,44]. GVP3 mix shows the highest
226 strength and dry bulk density of 12.60 MPa and 790-810 kg/m³, respectively, after 28 days of curing. Water absorption
227 of 32.5 – 48.6% is observed for GVP mixes after 24 h of immersion, with GVP3 showing the lowest water absorption
228 in comparison to other mixes. GVP12 shows an almost two-fold increase in water absorption in contrast to GVP3.
229 Like water absorption, the porosity of GVP mixes shows an upward trend with a higher amount of vermiculite in the
230 plasters. This gradual rise in the water absorption and porosity of plasters with addition of vermiculite is attributed to
231 the layered porous structure that entraps water molecules in the cavities [45]. The higher water absorption and porosity
232 limit the applicability of GVP only to interior building proposes. Therefore, we recommend the GVP3 mix for further
233 studies and the feasibility of commercial production.

234 **3.6 Durability Studies of Gypsum Vermiculite Plaster**

235 Different effects of environmental conditions on the plaster were investigated by durability studies. Winter and
236 summer like weather conditions created in the laboratory and performance of the GVP samples was studied by way
237 of compressive strength. For this hydrated sample of the plaster was exposed to extreme cold, heat & rain/humidity
238 (rain) and compressive strength was determined.

239 *3.6.1 Effect of Cold on the Performance of Gypsum Vermiculite Plaster*

240 The similar weather conditions as generally observed during winters in Roorkee (29°51' N; 77°53' E) were
241 achieved in the laboratory with the help of an environmental chamber. Atmospheric temperature in the day and night
242 in the January-March varies from 15 – 27 °C and 3 – 12 °C, respectively, with the low humidity of 70 – 75%. In order
243 to replicate the above conditions, the environmental chamber was maintained at a temperature of 18 – 20 °C during
244 the day and 3 – 5 °C in the night at a humidity of 70 – 75%, and the mechanical strength of the GVP3 was determined
245 after 7 days and 28 days of treatment. The compressive strength of GVP3 at 7 and 28 days is represented in Table 6.
246 Interpretation of results revealed a decrease in compressive strength (about 10 – 11%) of the plaster compared to the
247 strength attained by the plaster treated at 40 °C for the same period. A progressive increase in the strength development
248 of the plaster was noticed with an increase in the curing period without any variation in the weight of the plaster cubes
249 during the exposure test.

250 *3.6.2 Effect of Heat Exposure at High Temperatures*

251 In order to contemplate the effect of exposure of hydrated samples of GVP3 to high temperatures, 2.5 cm size
252 were placed in two different ovens maintained at 50 °C and 60 °C under 90% humidity. The compressive strength
253 values of the cubes were determined after 7 and 28 days of treatment in the respective ovens and results are shown in
254 Table 7. The perusal of results demonstrates a small increase in compressive strength of binders with an increase in

255 curing temperature. Around 5% and 7% gain in compressive strength was observed at 50 °C and 60 °C, respectively,
256 in contrast to the strength attained in hardening the plaster at 40 °C for the same period of time. [The water retentivity](#)
257 [of the cubes decreases due to the evaporation of the water at higher temperatures, hence it affects the strength of the](#)
258 [cubes.](#)

259 3.7 Sound Absorption

260 The normal incidence sound absorption coefficient vs. frequency of the GVP3 plaster is shown in Fig. 6a. In the
261 100 – 1500 Hz frequency range, sound absorption initially increases to a maximum of 0.65 at 400 Hz and then
262 decreases to 0.06 around 1300 Hz. In the higher frequency range 1500 – 4000 Hz, it shows a peak maxima (0.48) at
263 2500 Hz. However, the transmission loss vs. frequency plot (Fig. 6b) exhibits a zig-zag graph within the range of 30
264 – 45 dB, depicting the highest loss upto ~ 45 dB at 1600 Hz. These results suggest good insulation performance of
265 gypsum vermiculite plaster, GVP3. It may be due to the porous structure of plaster containing a large number of
266 interpenetrating interlinked pores that facilitates sound absorption and leads to noise reduction [42].

267 3.8 Efflorescence Studies

268 Efflorescence generally referred to the white powder generated at the surface of porous building materials [46].
269 It occurs due to the reaction of CO₂ in the atmosphere with hydroxide ions (OH⁻) that evaporate to the surface from
270 the core of the binder (Eqn. 8) and form carbonate salts with alkali metal ions [47]. The level of efflorescence in the
271 lightweight gypsum vermiculite plasters was measured by mixing 0.1% iron oxide pigment in the plaster mixes. The
272 pigment imparts red color to the plasters in order to clearly distinguish white patches of efflorescence developed on
273 the surface. Circular discs of diameter 10 cm and thickness 0.5 cm were casted and cured at 40 °C for a period of 28
274 days. The specimen discs were placed in a tray filled with water up to a height of 2.5 cm height and the water was
275 allowed to rise in the specimens, followed by drying at an ambient temperature. The test cycles were repeated for a
276 period of 3, 7 and 28 days and examined for any efflorescence produced in the same period. No efflorescence was
277 observed up to a period of 7 days. However, on the 28th day, slight efflorescence was observed on the edges of the
278 specimens.

279 3.9 Fire Evaluation and Thermal Conductivity Studies

280 Effect of fire on the performance of gypsum vermiculite plaster (GVP3) specimen was studied as per BS 476-
281 1997 (Part 7) [48]. This test evaluates the durability of the material in case of any accident of fire. Lateral spread of
282 flame along the surface of a specimen of a product orientated in the vertical position under opposed flow conditions
283 is measured, and materials are classified based on the rate and extent of the spread of flame. Specimens of size 900
284 mm x 270 mm x 07 mm were developed and the extent of flame spread after 1.5 min and after 10 min was determined.
285 The fire test results reveal that the GVP3 plaster is resistant to any susceptible fire accident as no spread of flames was
286 observed without any gas emission during the test. Based on the above findings, gypsum vermiculite plasters are
287 classified as Class I materials. Moreover, no loss of mechanical stability or any deformation was observed in the
288 specimen panel throughout the experiment.

289 Thermal conductivity gives an idea about the suitability of building materials for wall insulation applications and
290 is one of the most important parameter for insulating materials to be energy efficient. Thermal conductivities measured
291 for gypsum vermiculite plasters vary from 0.140 – 0.161 W/mK. GVP12 mix demonstrates the lowest conductivity of

0.140 W/mK and it increases as we decrease the amount of vermiculite in the mix, with GVP3 showing thermal conductivity of 0.161 W/mK. The thermal conductivity of gypsum vermiculite plasters exhibits good insulating properties with reference to some commercially available building materials such as brick tile, burnt clay brick, cement plaster and mortar [48]. The downfall trend of thermal conductivity in lightweight plasters is chiefly attributed to the lamellar structure of vermiculite that entraps a large volume of air, which reduces the thermal conductivity [49]. Larger the content of vermiculite in the mix, higher will be the porosity of the mix, which facilitates a larger volume of air that serves as an excellent insulator and leads to lower thermal conductivity values. Therefore, lightweight GVP are suitable materials for internal wall insulation with their substantial compressive strengths.

300

301 4. COST ESTIMATION

302 4.1 Cost of hemihydrate plaster using FGD gypsum

303	Cost of raw FGD gypsum per 1.33 tonne	= ₹1330/-	(\$16.41)
304	Cost of drying, grinding and calcination of FGD gypsum per tonne	= ₹2000/-	(\$24.68)
305	1.33 tonne of FGD gypsum gives	= 1.0 Tonne of POP	
306	Cost of retarder @₹400/kg	= ₹200 (0.50 kg/tonne)	(\$2.47)
307	Packaging per tonne @ 25bags of 40 kg	= ₹300/-	(\$3.70)
308			

309

310 **Cost of hemihydrate plaster per tonne** **Total = ₹3930/- (\$48.49)**

311 **DSR rates (CPWD) of POP per tonne** **= ₹5000/- (\$61.69)**

312

313 4.2 Cost of Gypsum Vermiculite Plaster (one tonne)

314	Cost of hemihydrate plaster @ ₹3530/-	= ₹3424/- (97 %)	(\$42.25)
315	Cost of Vermiculite per tonne @ 10000	= ₹300/- (3 %)	(\$3.70)
316	Blending & Packaging per tonne @ 25 bags of 40 kg	= ₹400/-	(\$4.94)
317			
318			

318

319 **Cost of Gypsum Vermiculite Plaster per tonne** **Total = ₹4124/Tonne (\$50.88)**

320 **Cost of Gypsum Vermiculite Plaster as per DSR** **= ₹6000/Tonne (\$74.03)**

321

322 The cost of the developed composite binder has been determined as per DSR as shown above. The rates gypsum
323 Vermiculite Plaster are less (₹4124/Tonne) as compared to the DSR rate (₹6000/Tonne). It is proved that the Gypsum
324 Vermiculite Plaster is also economically feasible construction material.

325

326 5. LIMITATION AND FUTURE SCOPE

327 **Limitation:** The water absorption of FGD gypsum is a little higher. Therefore, it cannot be used for external surfaces
328 and that is why it is recommended for internal applications.

329 **Future Scope:**

330 1. More and more utilization of by-product FGD gypsum, a waste generated from thermal power plants during the
331 desulphurization process, by developing a vermiculite-based composite binder.

332 2. Further, the aim of the study is to develop a lightweight low density interior textured plaster using vermiculite in
333 which paint is not required and no curing is needed.

334 6. Conclusion

335 The gypsum vermiculite plaster developed using waste gypsum shows good applicability for internal purpose. Several
336 mixtures were tried with different replacements of gypsum with vermiculite (3, 4, 5, 8, 10 & 12%). These plasters
337 show improved coverage and adhesion with dry weight less than half that of traditional sanded plaster. XRD analysis
338 confirms > 90% purity of FGD gypsum, with gypsum being the major phase in the pattern. SEM depicts the
339 agglomeration of vermiculite particles with FGD gypsum particles for strength generation. The strength of the GVP
340 was measured to be 5.5 – 12.6 MPa after 28 days of hydration, with GVP3 being the toughest. Gypsum vermiculite
341 plasters show high water absorption (32.5 – 48.6% at 24 h of immersion) and porosity due to the layered porous
342 structure of vermiculite present. GVP3 mix was selected as optimum composition as it exhibits the highest mechanical
343 strength and lowest water absorption. The performance of GVP3 under extreme cold and hold weather resulted in
344 good durability for the light weight plaster. These plasters provide reverberation (echo) control by absorbing sound
345 radiations with highest sound absorption coefficient observed of 0.65. There were no signs of efflorescence observed
346 in the plasters after 7 days. These materials were classified as Class I materials as no lateral spread of flame observed
347 nor any signs of deformation or gas emission. Thermal conductivities 0.140 – 0.161 W/mK were measured for GVP
348 that indicate towards excellent insulation behaviour of plasters. An economical and efficient way of waste mitigation
349 was devised to develop light weight plaster materials for interior applications exhibiting thermal as well as sound
350 insulation. This work can further be extended to reduce water absorption for exterior applications of these plasters.

351 Supplementary Information

352 The online version contains supplementary material available at <https://doi.org/xxxx>.

353 Acknowledgements

354 We are very thankful to the Director, CBRI Roorkee, for granting permission to publish this work.

355 Data Availability

356 The authors confirm that the data supporting the findings of this study are available within the article and its
357 supplementary materials.

358 References:

- 359 [1] P.S. Mangat, J.M. Khatib, L. Wright, Optimum utilisation of FGD waste in blended binders, Proc. Inst. Civ.
360 Eng. Constr. Mater. 159 (2006) 119–127. <https://doi.org/10.1680/coma.2006.159.3.119>.
- 361 [2] Z. Chen, S. Wu, F. Li, J. Chen, Z. Qin, L. Pang, Recycling of Flue Gas Desulfurization residues in gneiss
362 based hot mix asphalt: Materials characterization and performances evaluation, Constr. Build. Mater. 73
363 (2014) 137–144. <https://doi.org/10.1016/j.conbuildmat.2014.09.049>.
- 364 [3] Bakshi, P., Pappu, A., & Gupta, M. K. (2022). A review on calcium rich industrial wastes: a sustainable source
365 of raw materials in India for civil infrastructure-opportunities and challenges to bond circular economy.
366 Journal of Material Cycles and Waste Management, 24, 49–62.

- 367 [4] L. Coppola, G. Belz, G. Dinelli, M. Collepardi, Prefabricated building elements based on FGD gypsum and
368 ashes from coal-fired electric generating plants, *Mater. Struct. Constr.* 29 (1996) 305–311.
369 <https://doi.org/10.1007/bf02486365>.
- 370 [5] Tzouvalas, G., Rantis, G., & Tsimas, S. (2004). Alternative calcium-sulfate-bearing materials as cement
371 retarders: Part II. FGD gypsum. *Cement and Concrete Research*, 34(11), 2119–2125.
372 <https://doi.org/10.1016/j.cemconres.2004.03.021>.
- 373 [6] L. Coppola, G. Belz, G. Dinelli, M. Collepardi, Prefabricated building elements based on FGD gypsum and
374 ashes from coal-fired electric generating plants, *Mater. Struct. Constr.* 29 (1996) 305–311.
375 <https://doi.org/10.1007/bf02486365>.
- 376 [7] Koukouzas, N., & Vasilatos, C. (2008). Mineralogical and chemical properties of FGD gypsum from Florina,
377 Greece. *Journal of Chemical Technology and Biotechnology*, 83(1), 20–26. <https://doi.org/10.1002/jctb.1770>.
- 378 [8] E. Álvarez-Ayuso, X. Querol, Stabilization of FGD gypsum for its disposal in landfills using amorphous
379 aluminium oxide as a fluoride retention additive, *Chemosphere*. 69 (2007) 295–302.
380 <https://doi.org/10.1016/j.chemosphere.2007.03.062>.
- 381 [9] K.D. Ritchey, R.F. Korcak, C.M. Feldhake, V.C. Baligar, R.B. Clark, Calcium sulfate or coal combustion by-
382 product spread on the soil surface to reduce evaporation, mitigate subsoil acidity and improve plant growth,
383 *Plant Soil*. 182 (1996) 209–219. <https://doi.org/10.1007/BF00029052>.
- 384 [10] M.R. Tucker, Sulfur-nitrogen mix good for sandy soils, *North Carolina Farmer*. 12 (1993) 32.
- 385 [11] R.B. Clark, K.D. Ritchey, V.C. Baligar, Benefits and constraints for use of FGD products on agricultural land,
386 *Fuel*. 80 (2001) 821–828. [https://doi.org/10.1016/S0016-2361\(00\)00162-9](https://doi.org/10.1016/S0016-2361(00)00162-9).
- 387 [12] C. Leiva, C. García Arenas, L.F. Vilches, J. Vale, A. Gimenez, J.C. Ballesteros, C. Fernández-Pereira, Use of
388 FGD gypsum in fire resistant panels, *Waste Manag.* 30 (2010) 1123–1129.
389 <https://doi.org/10.1016/j.wasman.2010.01.028>.
- 390 [13] J. Li, X. Zhuang, C. Leiva, A. Cornejo, O. Font, X. Querol, N. Moeno, C. Arenas, C. Fernández-Pereira,
391 Potential utilization of FGD gypsum and fly ash from a Chinese power plant for manufacturing fire-resistant
392 panels, *Constr. Build. Mater.* 95 (2015) 910–921. <https://doi.org/10.1016/j.conbuildmat.2015.07.183>.
- 393 [14] L. Jiang, C. Li, C. Wang, N. Xu, H. Chu, Utilization of flue gas desulfurization gypsum as an activation agent
394 for high-volume slag concrete, *J. Clean. Prod.* 205 (2018) 589–598.
395 <https://doi.org/10.1016/j.jclepro.2018.09.145>.
- 396 [15] F.-Q. Zhao, H.-J. Liu, L.-X. Hao, Q. Li, Water resistant block from desulfurization gypsum, *Constr. Build.*
397 *Mater.* 27 (2012) 531–533. <https://doi.org/10.1016/j.conbuildmat.2011.07.011>.
- 398 [16] M. Garg, A.K. Minocha, N. Jain, Environment hazard mitigation of waste gypsum and chalk: Use in
399 construction materials, *Constr. Build. Mater.* 25 (2011) 944–949.
400 <https://doi.org/10.1016/j.conbuildmat.2010.06.088>.
- 401 [17] M. Garg, A. Pundir, Energy efficient cement free binder developed from industry waste—A sustainable
402 approach, *Eur. J. Environ. Civ. Eng.* 21 (2017) 612–628. <https://doi.org/10.1080/19648189.2016.1139510>.

- 403 [18] L.F. Vilches, C. Leiva, J. Olivares, J. Vale, C. Fernández, Coal fly ash-containing sprayed mortar for passive
404 fire protection of steel sections, *Mater. Construcción*, 55 (2005) 25–37.
405 <https://doi.org/10.3989/mc.2005.v55.i279.196>.
- 406 [19] Celik, A. G., Kilic, A. M., & Cakal, G. O. (2013). Expanded perlite aggregate characterization for use as a
407 lightweight construction raw material. *Physicochemical Problems of Mineral Processing*, 49(2), 689–700.
408 <https://doi.org/10.5277/ppmp130227>.
- 409 [20] Schackow, A., Effting, C., Folgueras, M. v., Güths, S., & Mendes, G. A. (2014). Mechanical and thermal
410 properties of lightweight concretes with vermiculite and EPS using air-entraining agent. *Construction and*
411 *Building Materials*, 57, 190–197. <https://doi.org/10.1016/j.conbuildmat.2014.02.009>.
- 412 [21] Rashad, A. M. (2016). Vermiculite as a construction material – A short guide for Civil Engineer. In
413 *Construction and Building Materials* (Vol. 125, pp. 53–62). Elsevier Ltd.
414 <https://doi.org/10.1016/j.conbuildmat.2016.08.019>.
- 415 [22] Shmuradko, V. T., Panteleenko, F. I., Reut, O. P., Panteleenko, E. F., & Kirshina, N. v. (2012a). Composition,
416 Structure, and Property Formation of Heat Insulation Fire-and Heat-Reflecting Materials Based on
417 Vermiculite for Industrial Power Generation. In *Refractories and Industrial Ceramics* (Vol. 53, Issue 8).
- 418 [23] Xie, N., Luo, J., Li, Z., Huang, Z., Gao, X., Fang, Y., & Zhang, Z. (2019). Salt hydrate/expanded vermiculite
419 composite as a form-stable phase change material for building energy storage. *Solar Energy Materials and*
420 *Solar Cells*, 189, 33–42. <https://doi.org/10.1016/j.solmat.2018.09.016>.
- 421 [24] Rashad, A. M. (2016). Vermiculite as a construction material – A short guide for Civil Engineer. In
422 *Construction and Building Materials* (Vol. 125, pp. 53–62). Elsevier Ltd.
423 <https://doi.org/10.1016/j.conbuildmat.2016.08.019>.
- 424 [25] Koksál, F., Gencil, O., & Kaya, M. (2015). Combined effect of silica fume and expanded vermiculite on
425 properties of lightweight mortars at ambient and elevated temperatures. *Construction and Building Materials*,
426 88, 175–187. <https://doi.org/10.1016/j.conbuildmat.2015.04.021>.
- 427 [26] Shmuradko, V. T., Panteleenko, F. I., Reut, O. P., Panteleenko, E. F., & Kirshina, N. v. (2012a). Composition,
428 Structure, and Property Formation of Heat Insulation Fire-and Heat-Reflecting Materials Based on
429 Vermiculite for Industrial Power Generation. In *Refractories and Industrial Ceramics* (Vol. 53, Issue 8).
- 430 [27] Gencil, O., del Coz Diaz, J. J., Sutcu, M., Koksál, F., Alvarez Rabanal, F. P., Martínez-Barrera, G., &
431 Brostow, W. (2014). Properties of gypsum composites containing vermiculite and polypropylene fibers:
432 Numerical and experimental results. *Energy and Buildings*, 70, 135–144.
433 <https://doi.org/10.1016/j.enbuild.2013.11.047>.
- 434 [28] Martias, C., Joliff, Y., & Favotto, C. (2014). Effects of the addition of glass fibers, mica and vermiculite on
435 the mechanical properties of a gypsum-based composite at room temperature and during a fire test.
436 *Composites Part B: Engineering*, 62, 37–53. <https://doi.org/10.1016/j.compositesb.2014.02.019>.
- 437 [29] Kumar, R., Srivastava, A., & Lakhani, R. (2022). Industrial wastes-cum-strength enhancing additives
438 incorporated lightweight aggregate concrete (Lwac) for energy efficient building: A comprehensive review.
439 In *Sustainability* (Switzerland) (Vol. 14, Issue 1). MDPI. <https://doi.org/10.3390/su14010331>.

- 440 [30] Singh, M., & Garg, M. (1999). Cementitious binder from fly ash and other industrial wastes. In *Cement and*
441 *Concrete Research* (Vol. 29).
- 442 [31] Gutiérrez-González, S., Gadea, J., Rodríguez, A., Blanco-Varela, M. T., & Calderón, V. (2012). Compatibility
443 between gypsum and polyamide powder waste to produce lightweight plaster with enhanced thermal
444 properties. *Construction and Building Materials*, 34, 179–185.
445 <https://doi.org/10.1016/j.conbuildmat.2012.02.061> Indian Standard, IS 1288 (1982). Methods of test for
446 mineral gypsum.
- 447 [32] Indian Standard, IS 1288 (1982). Method of test for mineral gypsum.
- 448 [33] Indian Standard, IS 12679 (1989). By-product gypsum for use in plaster, blocks and boards.
- 449 [34] M. Sutcu, Influence of expanded vermiculite on physical properties and thermal conductivity of clay bricks,
450 *Ceram. Int.* 41 (2015) 2819–2827. <https://doi.org/10.1016/j.ceramint.2014.10.102>.
- 451 [35] V. Meena, J. Malik, T.K. Mandal, Tri- α -PbO₂-Type Fe-Sb Tungstate by Topotactic Ion Exchange of
452 LiSbWO₆, *ACS Appl. Electron. Mater.* 3 (2021) 2504–2511. <https://doi.org/10.1021/acsaelm.0c01086>.
- 453 [36] F. Koksall, Y. Sahin, O. Gencel, Influence of expanded vermiculite powder and silica fume on properties of
454 foam concretes, *Constr. Build. Mater.* 257 (2020) 119547.
455 <https://doi.org/10.1016/j.conbuildmat.2020.119547>.
- 456 [37] Indian Standard, IS 2542 Part I (1978). Method of test for gypsum plaster, concrete and products: Plaster &
457 concrete.
- 458 [38] Indian Standard, IS 2547 Part II (1976). Gypsum building plaster: Premixed lightweight plaster.
- 459 [39] M. Garg, A. Pundir, Comprehensive study of fly ash binder developed with fly ash - Alpha gypsum plaster -
460 Portland cement, *Constr. Build. Mater.* 37 (2012) 758–765.
461 <https://doi.org/10.1016/j.conbuildmat.2012.08.018>.
- 462 [40] Indian Standard, IS 3346 (1980). Method of the determination of thermal conductivity of thermal insulation
463 materials (two slab guarded hot plate method).
- 464 [41] C. Martias, Y. Joliff, C. Favotto, Effects of the addition of glass fibers, mica and vermiculite on the mechanical
465 properties of a gypsum-based composite at room temperature and during a fire test, *Compos. Part B Eng.* 62
466 (2014) 37–53. <https://doi.org/10.1016/j.compositesb.2014.02.019>.
- 467 [42] O. Gencel, J.J. Del Coz Diaz, M. Sutcu, F. Koksall, F.P. Alvarez Rabanal, G. Martinez-Barrera, W. Brostow,
468 Properties of gypsum composites containing vermiculite and polypropylene fibers: Numerical and
469 experimental results, *Energy Build.* 70 (2014) 135–144. <https://doi.org/10.1016/j.enbuild.2013.11.047>.
- 470 [43] F. Koksall, O. Gencel, M. Kaya, Combined effect of silica fume and expanded vermiculite on properties of
471 lightweight mortars at ambient and elevated temperatures, *Constr. Build. Mater.* 88 (2015) 175–187.
472 <https://doi.org/10.1016/j.conbuildmat.2015.04.021>.
- 473 [44] L. Qi, J. Xu, K. Liu, Porous sound-absorbing materials prepared from fly ash, *Environ. Sci. Pollut. Res.* 26
474 (2019) 22264–22272. <https://doi.org/10.1007/s11356-019-05573-5>.
- 475 [45] C. Dow, F.P. Glasser, Calcium carbonate efflorescence on Portland cement and building materials, *Cem.*
476 *Concr. Res.* 33 (2003) 147–154. [https://doi.org/10.1016/S0008-8846\(02\)00937-7](https://doi.org/10.1016/S0008-8846(02)00937-7).

477 [46] J. Wang, T. Zhou, D. Xu, Z. Zhou, P. Du, N. Xie, X. Cheng, Y. Liu, Effect of nano-silica on the efflorescence
478 of waste based alkali-activated inorganic binder, *Constr. Build. Mater.* 167 (2018) 381–390.
479 <https://doi.org/10.1016/j.conbuildmat.2018.02.006>.

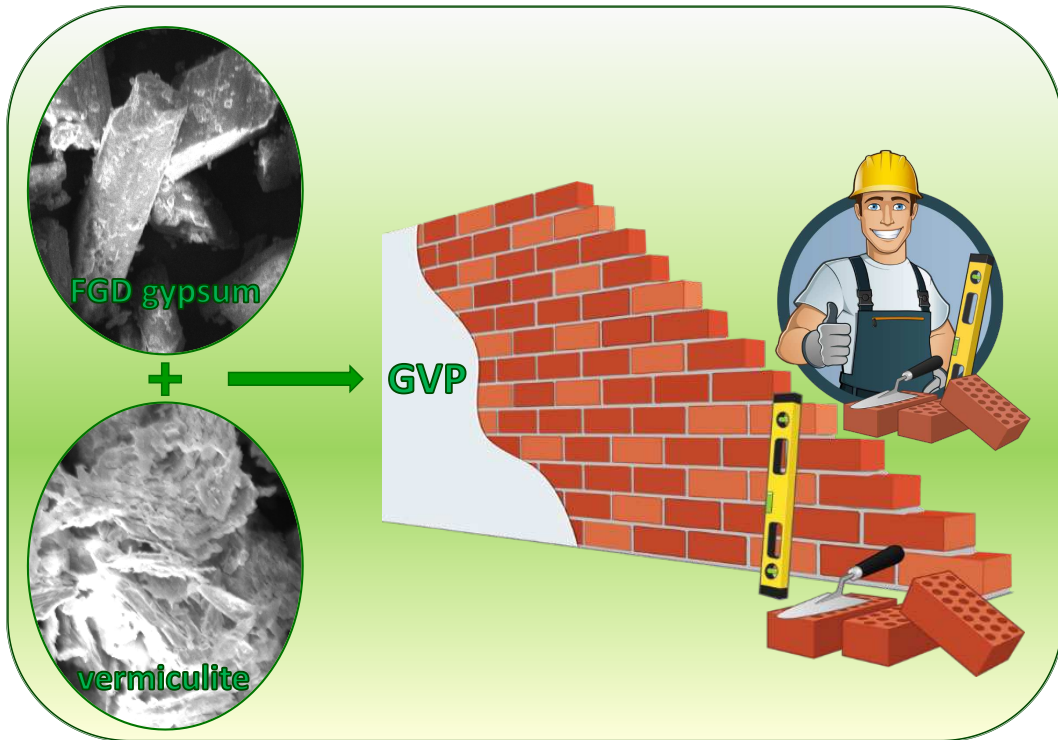
480 [47] British Standard, BS 476 Part 7 (1997). Method of classification of the surface spread of flame.

481 [48] A. Kumar, B.M. Suman, Experimental evaluation of insulation materials for walls and roofs and their impact
482 on indoor thermal comfort under composite climate, *Build. Environ.* 59 (2013) 635–643.
483 <https://doi.org/10.1016/j.buildenv.2012.09.023>.

484 [49] A.M. Rashad, Vermiculite as a construction material – A short guide for Civil Engineer, *Constr. Build. Mater.*
485 125 (2016) 53–62. <https://doi.org/10.1016/J.conbuildmat.2016.08.019>.

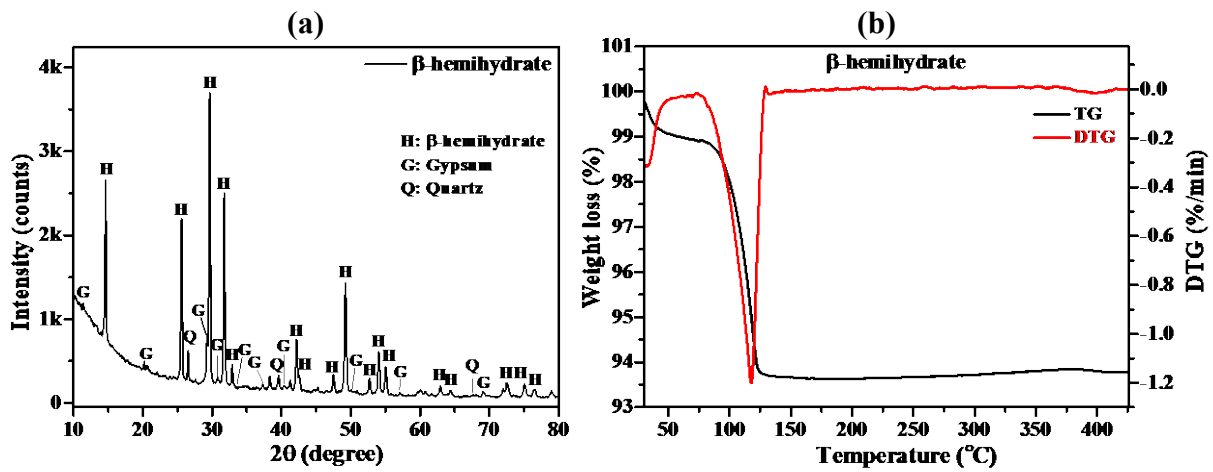
486
487
488
489
490
491
492
493
494
495
496
497
498
499
500
501

Graphical Abstract



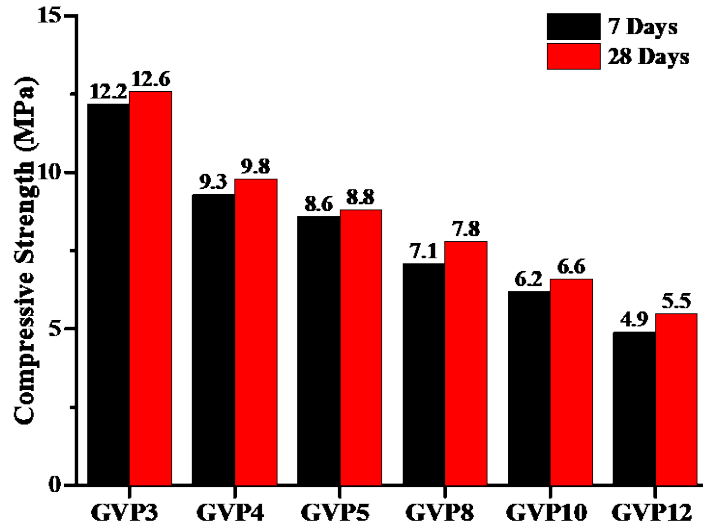
502
503
504

Figures



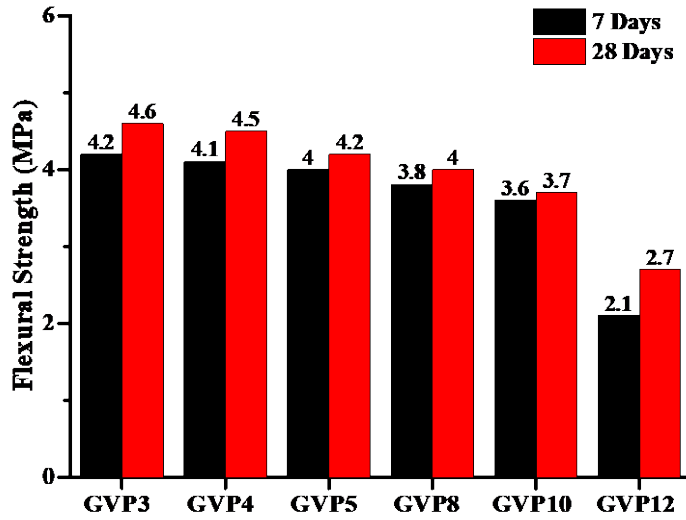
505
506
507

Fig. 1 (a) XRD pattern and (b) TG-DTG curves of β-hemihydrate obtained after calcination



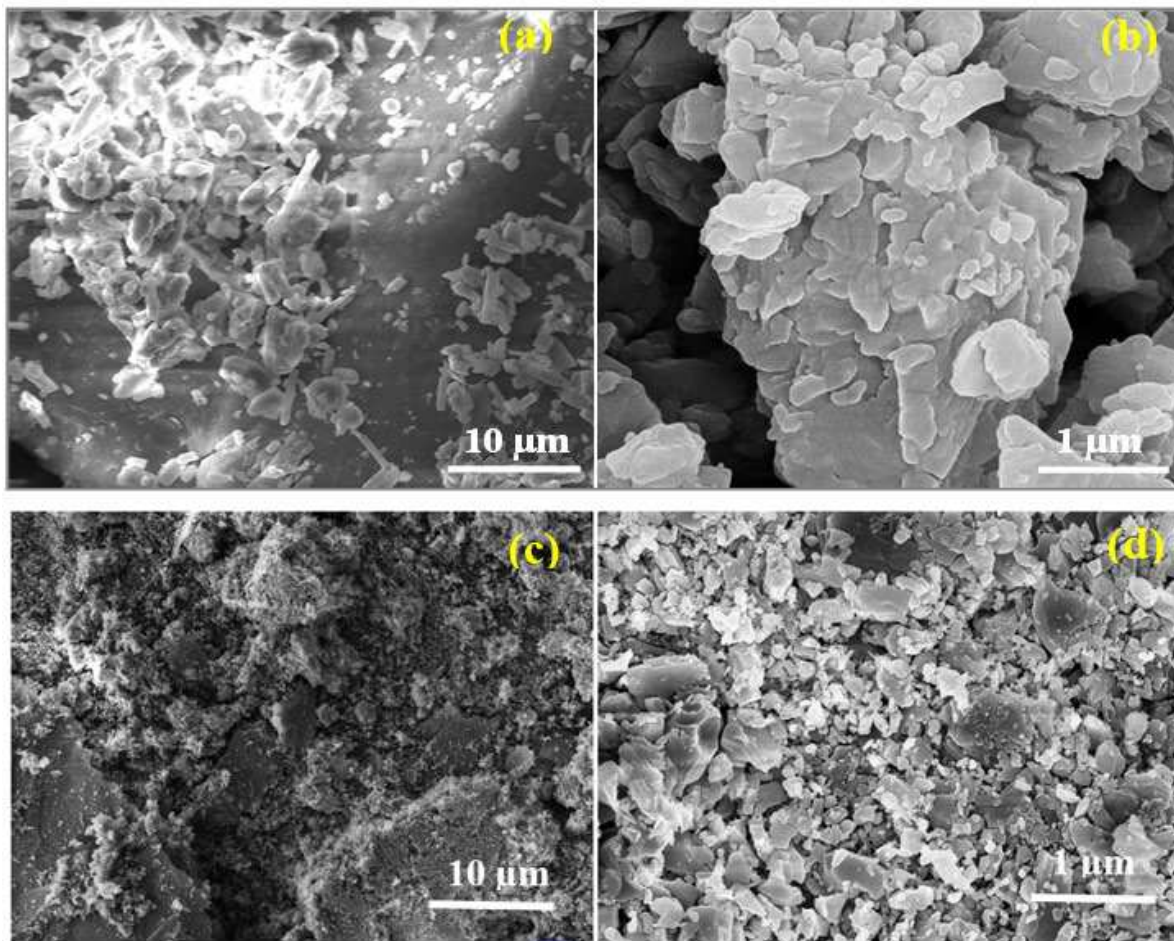
508
509
510

Fig. 2 Compressive strength results of GVP mixes at different hydration periods.

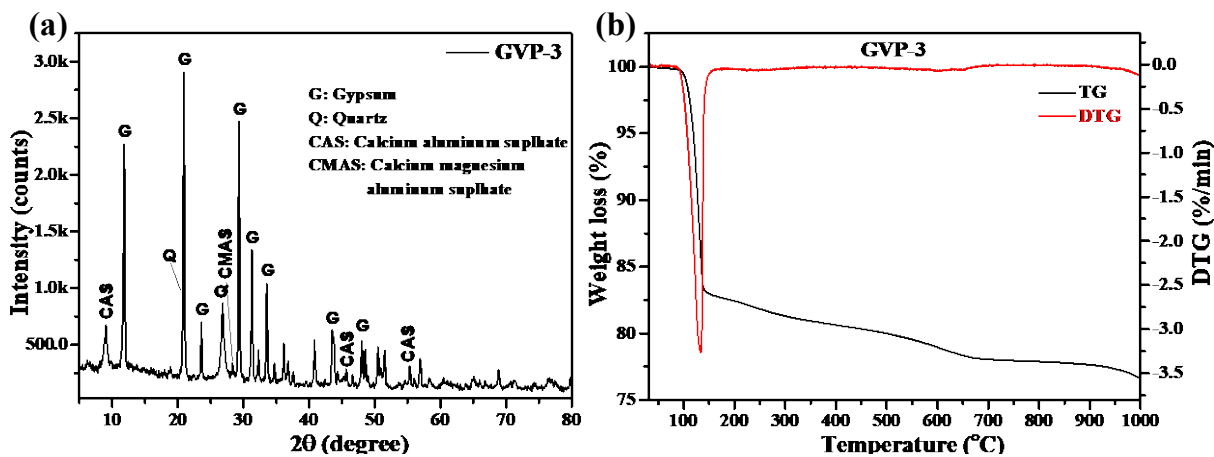


511
512

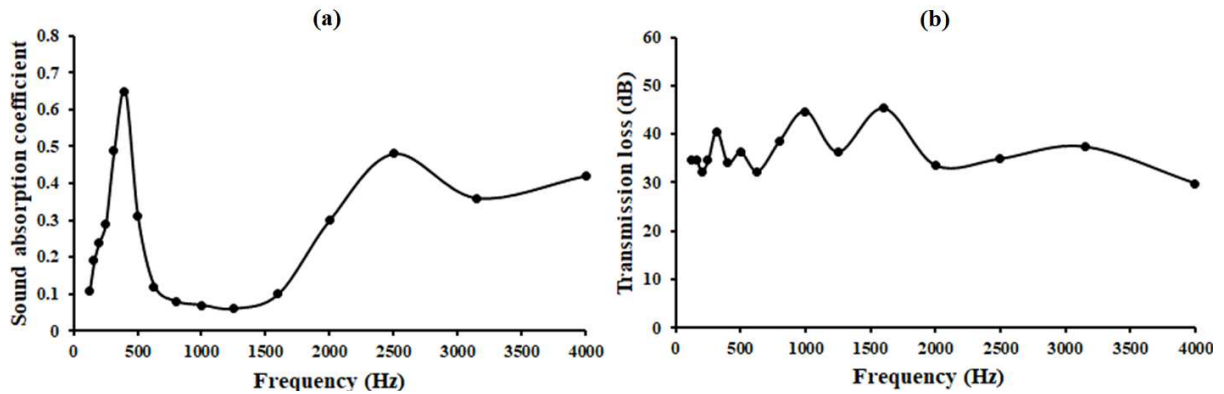
Fig. 3 Flexural strength results of GVP mixes at 7 days and 28 days of hydration.



513
 514 Fig. 4 SEM images of hydrated gypsum vermiculite plaster after 28 days of hydration GVP3 (a,b) and GVP12 (c,d)
 515



516
 517 Fig. 5 (a) XRD pattern and (b) TG-DTG curves of gypsum vermiculite plaster (GVP3) after 28 days of hydration.
 518



519
520 **Fig. 6** Normal incidence (a) sound absorption coefficient and (b) transmission loss of GVP3 plaster.
521
522

523 **Tables**

524 **Table 1. Physical properties of FGD gypsum and vermiculite.**
525

526

Parameters	FGDG	Vermiculite
pH	7.0 – 8.0	7.5 – 8.5
Moisture	10 – 12 %	6.0 – 8.0 %
Loss on ignition (LOI)	18 – 20 %	3.2 %
Specific Gravity	2.27	2.17
Bulk density	880-960 kg/m ³	200 – 220 kg/m ³
Specific Gravity	2.27	2.17
Specific Heat	----	0.84 – 1.08 KJ/kg.K
Bound water	18.2 %	----
Water holding capacity		220 – 320 % (w/w)
Fusion Point	----	1200 – 1320 °C
Sintering Temperature	----	1150 – 1250 °C
Particle size		1.0 – 2.0 mm
Passing 90 µm sieve	97 %	----
Passing 75 µm sieve	92 %	----
Passing 45 µm sieve	90 %	----

537
538 **Table 2. Mix compositions for development of Gypsum Vermiculite Plaster (GVP)**
539

Mix Designations	β-hemihydrate plaster (%)	Vermiculite (%)	Retarder (DTPA) (%)
GVP3	97.0	3.0	0.05
GVP4	96.0	4.0	0.05
GVP5	95.0	5.0	0.05
GVP8	92.0	8.0	0.05
GVP10	90.0	10.0	0.05
GVP12	88.0	12.0	0.05

540

Table 3. Physical properties of gypsum vermiculite plaster (GVP)

Parameters	Values					
	GVP3	GVP4	GVP5	GVP8	GVP10	GVP12
pH	7.40	7.38	7.35	7.30	7.28	7.26
Loss on ignition (LOI)	8.80 %	8.90 %	9.0 %	8.70 %	8.60 %	8.50 %
Dry Bulk Density (powder)	790 – 810 kg/m ³	770 – 790 kg/m ³	760 – 780 kg/m ³	750 – 760 kg/m ³	690 – 710 kg/m ³	640 – 660 kg/m ³
Set Bulk density of cube (dried at 42°C)	1370 – 1390 kg/m ³	1260 – 1280 kg/m ³	1210 – 1230 kg/m ³	1100 – 1120 kg/m ³	1010 – 1030 kg/m ³	1000 – 1010 kg/m ³
Specific gravity	2.17	2.12	2.07	1.96	1.86	1.76
Fineness: Retention on 45 µm sieve	8.0 – 12.0 %	8.0 – 12.0 %	8.0 – 12.0 %	10.0 – 15.0 %	10.0 – 15.0 %	10.0 – 15.0 %
Setting time	20 – 25 min	20 – 25 min	20 – 25 min	20 – 25 min	25 – 30 min	30 – 35 min

541

542

Table 4. Water absorption and porosity of gypsum vermiculite plaster (GVP)

Material	Water absorption (%)			Porosity (%)		
	2h	8h	24h	2h	8h	24h
GVP3	32.10	32.20	32.50	43.35	43.50	43.85
GVP4	34.60	34.60	35.00	43.20	43.20	43.70
GVP5	36.20	36.50	36.60	43.60	43.95	44.10
GVP8	38.70	38.85	39.20	40.30	40.40	41.20
GVP10	43.80	44.00	44.10	40.90	41.85	41.95
GVP12	47.15	48.20	48.60	42.40	43.40	44.05

543

544

Table 5. Compressive strength of GVP3 under exposed atmosphere during winter

545

546

547

Curing period	Compressive strength (MPa)
7 days	11.00
28 days	11.25

548

549

550

Table 6. Compressive strength of GVP3 under exposed atmosphere during summer

Curing period	Compressive strength (MPa)	
	50 °C	60 °C
7 days	12.75	13.00
28 days	13.20	13.50